Oxygen Regulation of a Nodule-Located Carbonic Anhydrase in Alfalfa[1]

Susana Gálvez, Ann M. Hirsch, Keith L. Wycoff[2], Stephen Hunt, David B. Layzell, Adam Kondorosi, and Martin Crespi*

Institut des Sciences Végétales, Centre National de la Recherche Scientifique, F–91198 Gif-sur-Yvette cédex, France (S.G., A.K., M.C.); Department of Molecular, Cell, and Developmental Biology, University of California, 405 Hilgard Avenue, Los Angeles, California 90095–1606 (A.M.H., K.L.W.); Queen's University, Kingston, Ontario, Canada K7L 3N6 (S.H., D.B.L.); and Institute of Genetics, Biological Research Center, Hungarian Academy of Sciences, Szeged, P.O. Box 521, H–6701 Szeged, Hungary (A.K.)

Control of the permeability to oxygen is critical for the function of symbiotic nitrogen fixation in legume nodules. The inner cortex (IC) seems to be a primary site for this regulation. In alfalfa (*Medicago sativa*) nodules, expression of the *Msca1* gene encoding a carbonic anhydrase (CA) was previously found to be restricted to the IC. We have now raised antibodies against recombinant *Msca1* protein and used them, together with antibodies raised against potato leaf CA, to demonstrate the presence of two forms of CA in mature nodules. Each antibody recognizes a different CA isoform in nodule tissues. Immunolocalization revealed that leaf-related CAs were localized primarily in the nitrogen-fixing zone, whereas the *Msca1* protein was restricted exclusively to the IC region, in indeterminate and determinate nodules. In alfalfa nodules grown at various O_2 concentrations, an inverse correlation was observed between the external oxygen pressure and *Msca1* protein content in the IC, the site of the putative diffusion barrier. Thus *Msca1* is a molecular target of physiological processes occurring in the IC cells involved in gas exchange in the nodule.

Carbonic anhydrase (CA; EC 4.2.1.1) catalyzes the reversible hydration of CO_2 to form HCO_3^-. Most reports on plant CAs are concerned with the enzyme from green tissues, but despite its abundance, the physiological role of this protein is still poorly understood (Sültemeyer et al., 1993; Badger and Price, 1994). In leaves two CA isoforms were localized to different subcellular compartments, the chloroplasts and the cytosol (Atkins et al., 1972; Fett and Coleman, 1994; Rumeau et al., 1996). In leaves of C_3 plants most of the CA activity resides within the chloroplast stroma. Thus it has been proposed that this enzyme accelerates the dehydration of bicarbonate to CO_2, providing a constant CO_2 supply for Rubisco activity during photosynthesis (Badger and Price, 1994; Majeau and Coleman, 1994). In C_4 leaves, however, CA is largely confined to the cytosol of mesophyll cells. The cytosolic enzyme phospho*enol*pyruvate carboxylase (PEPC; EC 4.1.1.31), which catalyzes the initial carboxylation reaction in C_4 photosynthesis, requires bicarbonate as a substrate instead of CO_2. In these plant tissues, CA and PEPC seem to be coordinately regulated, suggesting that the cytosolic-located CA may furnish the bicarbonate for PEPC activity (Hatch and Burnell, 1990; Ludwig et al., 1998).

Most of the CA-encoding cDNA clones so far identified have been isolated from green leaves (Burnell et al., 1990; Majeau and Coleman, 1991; Raines et al., 1992; Cavallaro et al., 1994; Fett and Coleman, 1994; Price et al., 1994). The only cDNA clone encoding a CA of a non-photosynthetic tissue was isolated from RNA of alfalfa (*Medicago sativa*) nodules (*Msca1*; Coba de la Peña et al., 1997). Nodules are symbiotic nitrogen-fixing organs that develop on legume roots under nitrogen-limiting conditions. In this symbiosis the bacterial partner fixes atmospheric nitrogen to form ammonium, which is then exported into the plant cell. In exchange, the plant partner provides a carbon source to the nitrogen-fixing bacteroid forms to sustain their metabolism. Hence a coordination of carbon and nitrogen metabolisms is required for nodule function (Vance and Gantt, 1992).

In legume nodules PEPC plays an important role in the anaplerotic replenishing of the Krebs cycle intermediates that are removed to provide either the carbon skeletons for ammonia assimilation (Vance et al., 1994), or the organic acids used by bacteroids for carbon metabolism and N_2 fixation (King et al., 1986). In nodules grown under normal oxygen conditions Suc coming from photosynthesis is metabolized via glycolysis to form phospho*enol*pyruvate. In the presence of CA and PEPC, this phospho*enol*pyruvate is

[1] This work was supported by the European Union Biotechnology program FIXNET (no. PL962319 to S.G.) and by the U.S. Department of Agriculture-National Research Initiation Competitive Grants Program (no. 92–37305–2366 to K.L.W.). Additional support came from the Natural Sciences and Engineering Research Council (Canada to D.B.L.) and from the National Science Foundation (no. 90–23888 to A.M.H.).

[2] Present address: Planet Biotechnology, 2461 Wyandotte Street, Mountain View, CA 94043.

* Corresponding author; e-mail crespi@isv.cnrs-gif.fr; fax 33–1–69823695.

transformed into oxaloacetate and malate. Both enzymatic activities are present in these organs (Atkins, 1974; Vance et al., 1994). Dark CO_2 fixation by PEPC in legume nodules occurs at rates equivalent to leaves of C_4 plants, accounting for the fact that PEPC can represent up to 2% of the total soluble protein in nitrogen-fixing cells (Miller et al., 1987).

Symbiotic nitrogen fixation depends upon nitrogenase, an O_2-labile enzyme located within bacteroids. However, bacteroid nitrogenase requires a large supply of ATP generated through oxidative phosphorylation. Hence the plant must provide the bacteria with a high O_2 flux at a low O_2 concentration. The plant exercises then a physiological control over the nodule's permeability to O_2 diffusion (Hunt and Layzell, 1993). Microelectrode studies (Witty et al., 1986) demonstrated the presence of steep O_2 concentration gradients between the cortex and the central tissues of legume nodules; the concentration in infected cells (10–50 nM; Kuzma et al., 1993) is about 10^{-4} of that at the nodule surface (250 μM). Although oxygenated leghemoglobin gradients may have a role in the fine control of infected cell O_2 concentration (Thumfort et al., 1999), a physical barrier to gas diffusion in the inner cortex (IC) seems to be the primary site for the regulation of nodule permeability to gas diffusion (Hunt and Layzell, 1993).

Nodule permeability to oxygen is controlled by two distinct mechanisms: long-term developmental adaptations, such as changes in the number of IC cell layers, and short-term physiological mechanisms allowing rapid adjustments to changes in oxygen and other environmental parameters (Hunt and Layzell, 1993). The mechanisms responsible for controlling short-term oxygen diffusion remain poorly understood, but most likely involve changes in the gas-to-liquid composition in the path that O_2 (and other gases) take in diffusing into (or out of) the nodule. In long-term developmental regulation of nodule permeability, proteins exclusively present in the nodule IC may play a role in this process. In alfalfa, nodules grown at high oxygen concentrations showed increased amounts of a glycoprotein that bind to the monoclonal antibody MAC236 (Wycoff et al., 1998). This glycoprotein was present in the intercellular spaces of the IC where it could contribute to their occlusion, thereby reducing permeability to O_2 diffusion. Because expression of the *Msca1* gene was detected in the nodule IC in nitrogen-fixing and ineffective nodules (Coba de la Peña et al., 1997), the function of *Msca1* is not likely to be related to nitrogen fixation or malate supply to the bacteroids.

To assess the role of *Msca1* in legume nodules, the present study characterized the localization of two forms of CA in determinate and indeterminate nodules, from *Lotus japonicus* and *Medicago truncatula*, respectively. Then using alfalfa indeterminate nodules, the effect of rhizosphere O_2 concentration was examined on the expression of the *Msca1* isoform in the nodule IC. The results of these experiments have led to proposals for the physiological role of *Msca1* in legume nodules.

RESULTS

Mature Nodules Contain at Least Two Forms of CA Located in Different Cell Types

We have previously identified *Msca1*, a cDNA encoding an alfalfa CA expressed in nodule tissues (Coba de la Peña et al., 1997). In mature nodules, the corresponding transcripts were detected in a thin layer of cells situated in the IC region at the nodule periphery. To localize the protein in nodules, a recombinant His-tagged *Msca1* protein purified from a bacterial culture was used to raise polyclonal antibodies in rabbits. The specificity of these antibodies was tested by western-blot analysis of total soluble protein extracts from roots, nodules, and leaves (Fig. 1A). In nodule extracts, these antibodies strongly recognized a single protein band with a molecular mass of 28.5 kD, very close to that expected for the putative *Msca1*-encoded protein. They did not recognize any root protein, but in leaf extracts, a protein band of 39.5-kD cross-reacted. This molecular mass was close to the size range described for leaf CA monomers (27–36 kD; Majeau et al., 1994; Rumeau et al., 1996).

Antibodies raised against a synthetic peptide corresponding to the N-terminal amino acid sequence of the potato leaf chloroplastic CA (kindly provided by G. Peltier) were also tested in western blots. These antibodies cross-reacted also with the cytosolic potato leaf isoform (Rumeau et al., 1996). However, this peptide region is not conserved in the *Msca1*-encoded

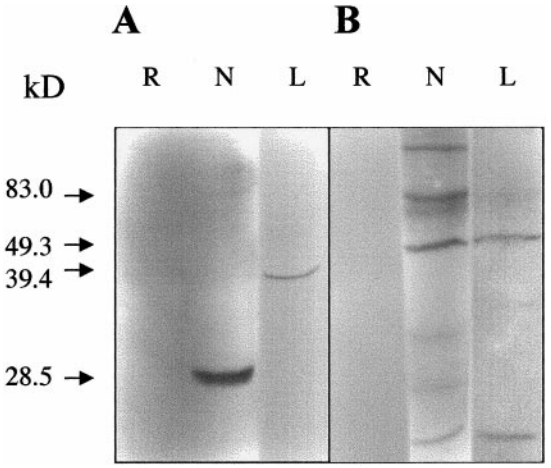

Figure 1. Western-blot analysis for detecting CA in *M. truncatula* protein extracts. Proteins were separated by SDS-PAGE, electrotransferred onto nitrocellulose, and incubated with antibodies raised against either the recombinant *Msca1* protein (A) or the potato leaf CA (B). Forty micrograms of total soluble proteins from roots (R), mature nodules (N), and leaves (L) were loaded per lane. Arrows indicate the major protein bands recognized by the antibodies.

protein and in *M. truncatula*, they failed to recognize any protein band in total root extracts (Fig. 1B). They did, however, cross-react with at least four nodule proteins (two bands of 83 and 49.3 kD and two bands of high and very low molecular mass), but not with the *Msca1* band. In leaf extracts, two bands were revealed (the one having a very low molecular mass is probably a degradation product), but not the 39.4-kD isoform that is related to *Msca1*. The protein bands recognized by the potato anti-CA antibodies have the same molecular mass as two of the nodule proteins. To confirm that these antibodies recognized CA isoforms in nodules an assay of CA activity in gel was carried out (Tashian, 1969). In native gels two CA isoforms were detected in leaves and nodules (Fig. 2A). The leaf and anti-*Msca1* antibodies recognized the upper and lower bands, respectively, whereas the latter antibody did not recognize any active band in the leaf extracts (Fig. 2B). On the other hand, the recombinant *Msca1* protein was not recognized by the leaf antibodies (Fig. 2C). Hence in mature nodules, there are at least two forms of CA: one is recognized by the anti-*Msca1*-encoded protein antibodies, and other form(s) cross-react with the anti-potato leaf CA antibodies.

We next addressed where these different isoforms are located in nitrogen-fixing nodules (Fig. 3). We carried out an immunolocalization analysis on mature *M. truncatula* nodules with either the pre-immune serum or the anti-*Msca1* protein antibodies (Fig. 3, A–C). A secondary antibody linked to the Cy3 fluorophore was used for revealing the immunological signal. The *Msca1* antibodies strongly labeled a thin region at the periphery of the nodule equivalent to the IC, whereas no significant signal was detected in the nitrogen-fixing central region (Fig. 3C). This binding of anti-*Msca1* antibodies was blocked by preincubation with the recombinant *Msca1* protein (data not shown). Moreover, in determinate nodules of *L. japonicus*, a similarly strong signal was observed in the IC cells (Fig. 3, G and H). This suggests that *Msca1* proteins are specifically located in the inner cortical cells in indeterminate and determinate nodules. A similar immunolocalization experiment was carried out using the anti-potato leaf CA antibodies (Fig. 3, D–F, I). In *M. truncatula*, no signal was detected in the IC region, but was found mainly in the central region (compare Fig. 3, C and F). In mature nodules from *L. japonicus*, incubation with the leaf CA antiserum also labeled all cells containing nitrogen-fixing bacteroids (Fig. 3I). Noninfected cells, likely implicated in metabolite exchange mechanisms, lacked any label regardless of their location. The nodule periphery did not contain any leaf-related CA isoform in indeterminate or determinate nodule types.

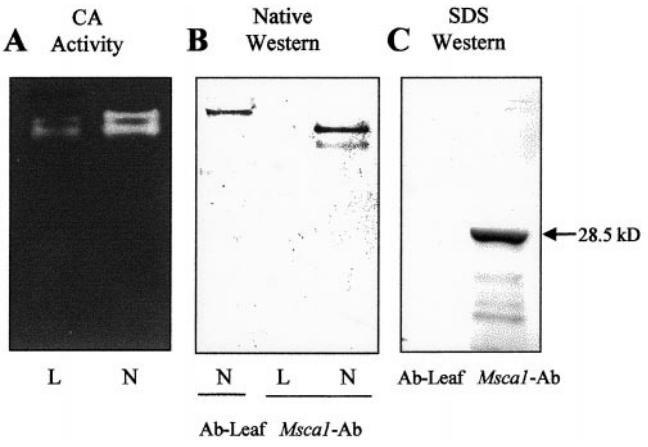

Figure 2. Detection of enzymatic isoforms of CA in nodule tissues. A, Total leaf (L, 100 μg) and nodule (N, 5 μg) extracts were analyzed in native gels and processed for in gel detection of CA enzymatic activity using veronal buffer. B, Parallel native gels were transferred to nitrocellulose and incubated with anti-leaf CA (Ab-Leaf) or anti-*Msca1* antibodies (*Msca1*-Ab) as indicated. C, Western SDS-PAGE blots containing total extracts (20 μg) of *Escherichia coli* cells expressing recombinant *Msca1* (28.5 kD) were probed with anti-leaf CA and anti-*Msca1* antibodies, left and right, respectively.

These results indicate that in mature nodules at least two CA isoforms located in different cell types (IC or infected cells) exist, suggesting that they may have different, noninterchangeable physiological roles in nodule metabolism. The CA recognized by the anti-leaf CA antibodies is likely to be involved in the provision of bicarbonate to PEPC, for the synthesis of carbon skeletons needed for ammonia assimilation and bacteroid respiration. The other CA isoform, the *Msca1*-encoded protein, is present in the IC, a region of the mature nodule proposed to be involved in the control of oxygen diffusion inside the nodule, and may have a very different primary function.

The presence of high amounts of CA protein(s) inside the nitrogen-fixing region of the nodule explains why Coba de la Peña et al. (1997) measured minor changes of CA activity in extracts of young and mature nodules, whereas there was a large variation in the *Msca1* mRNA amounts and localization when the two samples were compared. The CA forms present in nodules are different enough in nucleotide and protein sequences so that they do not exhibit cross-hybridization at mRNA or immunological levels, although both contribute to the measured CA activity. In consequence, measurement of CA enzymatic activity in mature nodules is not appropriate for studying the physiological role of the *Msca1*-related protein. Thus a strategy involving the use of isoform-specific antibodies in an immunolocalization approach was undertaken.

Effect of External Oxygen Pressure on *Msca1* Protein Levels

A variable diffusion barrier, located at the level of the IC region, has been proposed to control the entry of oxygen into the central infected zone (IZ; Witty et al., 1986; Batut and Boistard, 1994). However, the

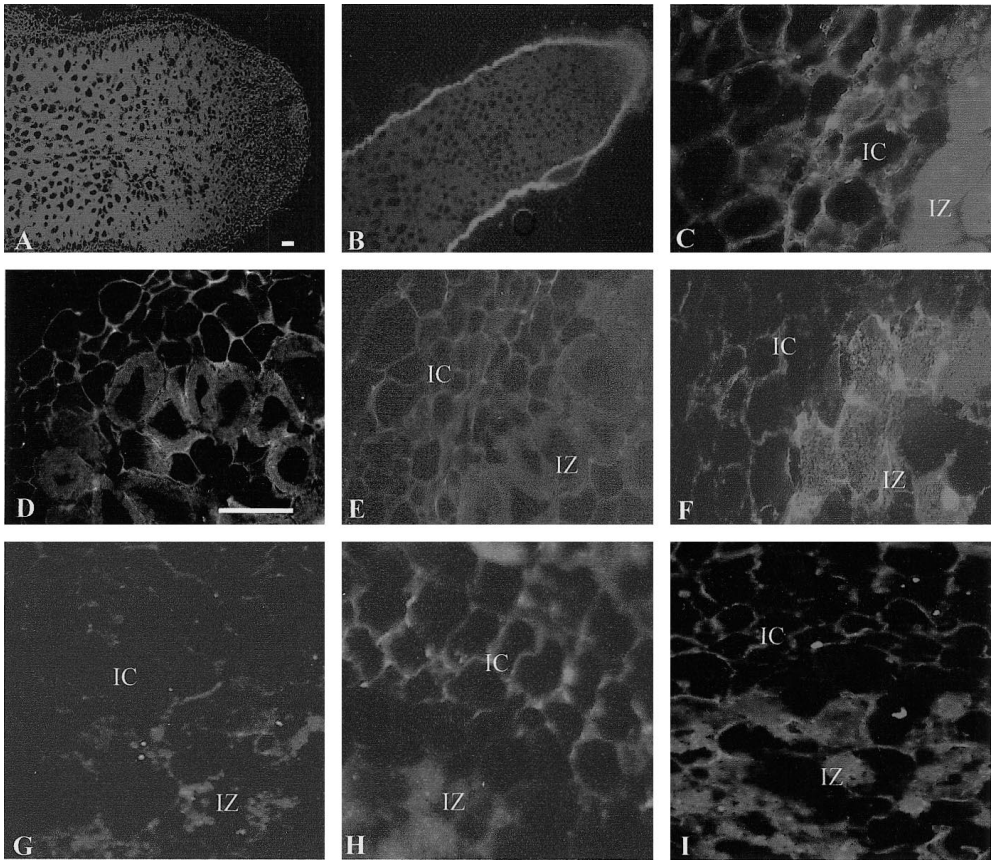

Figure 3. Immunolabeling of CA isoforms in mature nodules. After incubation of sections from *M. truncatula* (A–F) and *L. japonicus* (G–I) nodules with either the pre-immune serum (A, E, and G), the anti-*Msca1* antibodies (B, C, and H), or the anti-leaf CA antibodies (F and I), detection was based on Cy3 fluorescence. A, Pre-immune serum control section indicating the absence of specific labeling in the IC in paraffin-embedded nodules. B, A section similar to A was incubated with anti-*Msca1* antibodies. C, Detail of the IC region in B is shown. Red fluorescence labels the IC cells. D, Autofluorescence of a nodule showing the infected and IC cells. E, Pre-immune serum control section of a similar region. F, Same section as D incubated with anti-leaf CA antibodies. Red fluorescence indicates that CA recognized by these antibodies are located in the nitrogen-fixing zone and not in the IC-region. G through I, Detail of consecutive sections of *L. japonicus* nodules incubated with pre-immune serum (G), anti-*Msca1* antibodies (H), and anti-leaf antibodies (I). Red fluorescence labels mainly the IC or IZ region in H and I, respectively. A and B, Paraffin-embedded material. C through I, Methacrylate-embedded material. Bars = 50 μm.

elements involved in the formation and maintenance of this barrier are unknown. Changes in the external oxygen pressure evoke adjustments in the thickness and shape of the IC cells, as well as in the occlusion of their intercellular spaces (Arrese-Igor et al., 1993; Iannetta et al., 1995). To study whether the *Msca1*-encoded CA isoform is implicated in the control of oxygen diffusion inside the nodule, immunolocalization assays on mature nodules of alfalfa grown under different oxygen pressures were carried out. The effects of these changes in oxygen concentration on nodule structure and gas-exchange measurements have been characterized previously (Wycoff et al., 1998).

Longitudinal sections of these nodules were incubated in the presence of either a pre-immune serum or antibodies raised against the IC-located CA, as described above (Fig. 4). The autofluorescence of the nodules was used to identify the different cell types (Fig. 4, A–C). To compare relative intensities of red fluorescence between different treatments, serial sections of the same nodule localized on the same slide were incubated with either the pre-immune serum (Fig. 4, D–F) or with the anti-CA antibodies (Fig. 4, G–L). In this way the observed differences were due exclusively to the primary antibody, and not due to artifacts brought about by using different nodules or slides.

Nodules grown under normal oxygen pressure (21%; Fig. 4, H and K) had a detectable amount of *Msca1* protein in the IC. Nodules grown at subambient oxygen concentration (8%) showed significantly increased *Msca1*-related signal in this region (Fig. 4, G and J). In a converse manner, nodules grown at high (50%) O_2 exhibited an almost undetectable amount of specific labeling in the IC (Fig. 4, I–L).

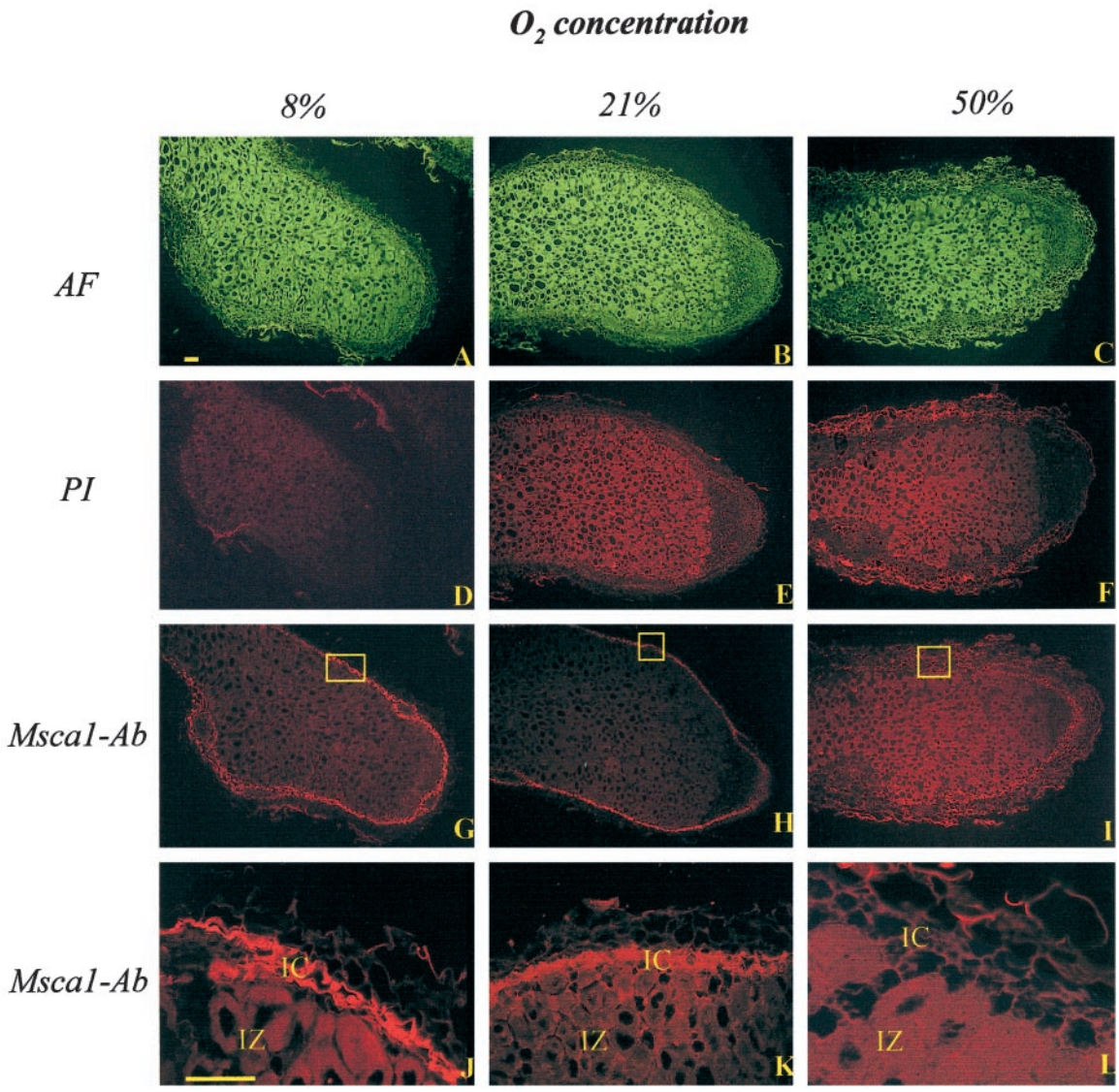

Figure 4. Immunolabeling of the IC-located *Msca1* protein in alfalfa mature nodules grown under different oxygen concentrations. Sections from paraffin-embedded nodules grown at 8% O_2 (A, D, G, and J), 21% O_2 (B, E, H, and K), or 50% O_2 (C, F, I, and L) were incubated with either the pre-immune serum (PI) or the anti-*Msca1* antibodies (*Msca1*-Ab). The immunological signal was revealed by incubation with a secondary antibody linked to the Cy3 fluorochrome. Autofluorescence (AF) revealed nodule morphology (A through C). J and L are magnifications of the boxed areas in G and I, respectively. Bars = 50 μm.

Fifteen slides containing around 30 sections per slide, corresponding to five to six different nodules per treatment were tested and gave identical results. These results strongly suggested that the external oxygen pressure had an effect on *Msca1* protein content in the IC. In the 21% and 50% samples, a background signal in the central region of the nodule was detected with the pre-immune serum. The signals obtained with the anti-*Msca1* antibodies in the central region were not at significantly higher level than this background, preventing us from detecting any change in *Msca1* protein content in the central cells.

Differences were quantified for four nodules (deposited on different slides) using confocal microscopy. The intensity of labeling (arbitrary units) per surface unit (micromoles^2) was calculated for each section at the levels of the IC (specific *Msca1*-related signal) and the IZ allowing us to deduce the relative increase in the red signal for each treatment. The results are shown in Table I. For nodules grown under normal oxygen pressure, *Msca1* IC-related level was taken as 100%. Nodules grown under 8% O_2 exhibited a 3-fold increase, whereas no significant difference in signal from nodules grown in 21% O_2 was detectable in the IC of nodules grown under 50% O_2. Hence an inverse correlation between *Msca1* amounts in the IC and the external oxygen pressure was demonstrated.

Table I. *Fluorescent quantification of the IC-located Msca1 protein in nodules grown under different oxygen pressures*

$[O_2]$	Preimmune Serum		Anti-*Msca1* Antibodies	
	Intensity/Surface[a]		Intensity/Surface	IC-related signal[c]
		a.u./μm²		
8%	IC[b]	300 ± 30	524 ± 31	281%
	IZ	312 ± 19	288 ± 14	
21%	IC	274 ± 13	267 ± 13	100%
	IZ	317 ± 2	183 ± 16	
50%	IC	212 ± 19	271 ± 16	n.s.[d]
	IZ	201 ± 23	273 ± 6	

[a] Values obtained for the intensity of fluorescence per unit area are expressed in arbitrary units (a.u./μm^2). [b] Values (mean ± SD) were obtained per duplicate for four nodules from samples incubated with either the preimmune serum or the anti-*Msca1* antibodies. [c] C-related signal was determined by subtracting IC-IZ fluorescence values and considering the 21% oxygen sample as 100%. [d] n.s., No significant difference from IZ background.

DISCUSSION

The results presented in this paper show that in mature nodules the *Msca1*-encoded protein is located in the IC region of nodules and its concentration is strongly influenced by the external oxygen pressure. We proposed two possible explanations for the observed inverse relationship between growth O_2 concentration and *Msca1* in the IC. Both explanations are based on observations from previous structural analyses of nodules grown under 1% or normal O_2 concentrations. These studies showed two major differences at the level of the IC: in nodules grown under hypoxic conditions, the inner cortical cells had a larger volume size than in normal nodules, and the intercellular spaces were mostly unoccluded (Arrese-Igor et al., 1993). Because the diffusion coefficient of the oxygen in air is 10,000 times higher than in water, these morphological variations of the IC cells, possibly related to changes in their osmolarity, regulate the diffusion of the oxygen into the nodule (Hunt et al., 1990; Layzell et al., 1990; Vessey and Waterer, 1992).

A first explanation is based on the assumption that in IC cells the factors affecting osmoregulation of cell volume are similar to those acting in the leaf guard cells. In these cells, malate synthesized through PEPC activity is taken up by the vacuole, provoking water influx into the guard cells, which leads to stomatal opening. Malate uptake depends on specific transporters whose activities are essential for the initial increase in turgor. However, guard cell tonoplasts also contain another kind of transporter, the so-called slow-vacuolar channels that are able to transport a large range of substances (including malate) in an unspecific way. It has been proposed that in plants exhibiting crassulacean acid metabolism, these channels could be responsible for malate release during daytime (Iwasaki et al., 1992).

Based on this we can infer that in IC cells osmolarity is also regulated through a constant supply of malate. This reversible osmocontraction may then lead to the alteration of oxygen permeability in the nodule (Drevon et al., 1995; Pathirana et al., 1997). The results presented here allow us to propose as a first hypothesis that *Msca1* in the IC cells (Fig. 5) may limit bicarbonate availability to PEPC for malate production. In this way *Msca1* will affect cell volume and turgor. In nodules grown under hypoxic oxygen pressure the amount of *Msca1* protein in the IC cells was higher than in normal nodules (Fig. 4; Table I), suggesting that PEPC activity yields a maximal amount of malate that can be taken up by the vacuole. The higher CA activity might be needed to maintain a continuous supply of malate. Thus, low oxygen pressure leads to increased cell osmotic potential, water influx, increased cell turgor, and increased oxygen diffusion through the IC region (Fig. 5, A and B). In contrast, nodules grown under a supra-ambient oxygen pressure, having almost undetectable *Msca1* protein levels in their IC cells (Fig. 4; Table I), may not have sufficient bicarbonate to sustain PEPC activity and malate supply, and thus less water would be taken up osmotically into the cell. Instead a diminution in soluble sugars would induce water efflux from the cell decreasing its volume and the intercellular spaces, rendering the diffusion of oxygen into the nodule more difficult (Fig. 5C). Therefore, *Msca1* function may be linked to the control of oxygen permeability in nodules.

Our alternative explanation is that the *Mscal* protein may be involved in facilitating diffusion of CO_2 across an aqueous diffusion barrier. Modeling studies (Sheehy et al., 1987; Hunt et al., 1988) have indicated that because of the greater solubility of CO_2 than O_2 in water, CO_2 can diffuse out of the nodule more readily than O_2 enters it. As a result, a partial

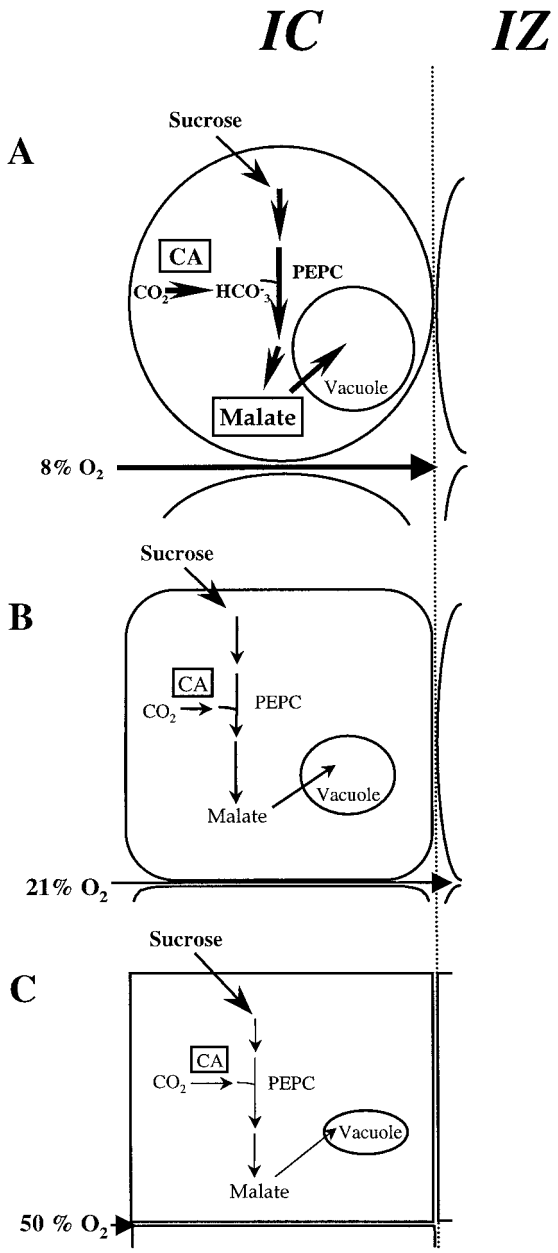

Figure 5. Role of *Msca1* in the IC cells of mature nodules. Under normal oxygen conditions (21%; B), CA activity assures malate production. Under hypoxia (8%; A), nodules contain more CA protein in the IC increasing malate production and, concomitantly, their water uptake and cell volume. The resulting increase of the number and volume of intercellular spaces facilitates oxygen diffusion inside the nodule. Nodules grown under supra-ambient oxygen pressure (50%; C) have less CA in the IC cells, suggesting that bicarbonate amounts may not be sufficient to sustain PEPC activity and malate production. A decrease in cell volume renders oxygen diffusion into the nodule more difficult.

vacuum can be formed within the nodule that would draw the gas of the nodule rhizosphere into the central zone by mass flow of air (as distinct from diffusion). This vacuum effect is similar to the concept of convective gas flow described for some aquatic plants (Beckett et al., 1988). In nodules it may be instrumental in increasing the flux of O_2 to the IZ, thereby supplementing the O_2 diffusion, which would occur across the water-filled cells of the IC. The magnitude of the vacuum would be dependent on the flux of CO_2 across the cells of the IC, a flux greatly facilitated by bicarbonate. Bicarbonate/CO_2 equilibrium might be controlled by *Msca1*-catalyzed reactions.

In nodules grown at a low O_2 concentration the partial vacuum generated by bicarbonate-facilitated CO_2 transport could play a major role in supplying O_2 to the infected cells, thereby accounting for the high levels of the *Msca1* protein in the IC of these nodules. In nodules grown at high oxygen concentrations there are more cell layers in the IC and gas-filled intercellular spaces across IC layers may be rare or nonexistent (Arrese-Igor et al., 1993). In such nodules an atmospheric pressure gradient across the nodule would not draw O_2 into the central zone by mass flow, so there would be little advantage for the nodule to enhance CO_2 efflux by CA-catalyzed facilitated diffusion. This could explain the low amount of *Msca1* in the nodules at 50% O_2. Thumfort (1996) recently modeled the effect of bicarbonate/CO_2 equilibrium on convective gas flow into legume nodules and concluded that it would enhance O_2 transport into the central zone.

Both explanations are consistent with the suggestion that the *Msca1* protein is an early molecular target of physiological processes occurring in the inner cortical cells dealing with the control of nodule gas exchanges. Further analysis of these hypotheses will be attempted in our laboratory by using transgenic *M. truncatula* plants affected in *Msca1* function.

MATERIALS AND METHODS

Plant and Bacterial Material and Plant Growth

Medicago truncatula seeds (ecotype 108) were sterilized by treatment with a 0.2% (w/v) sodium hypochlorate solution for 3 h at 30°C, washed, and germinated on 1% (w/v) water/agar plates for 2 d in the dark plus 2 weeks in the light. Seedlings were then transferred to aeroponic tanks and cultured in a minimum medium as described previously (Crespi et al., 1994). After 2 weeks plants were inoculated with the bacterial strain (*Sinorhizobium meliloti Sm*41) as described previously (Crespi et al., 1994). Mature *M. truncatula* nodules were collected 3 weeks after infection.

Growth conditions of alfalfa (*Medicago sativa*) plants under different oxygen partial pressures as well as the histological characterization of the resulting nodules have been described (Wycoff et al., 1998). *Lotus japonicus* plants grown in the greenhouse for 5 weeks under low combined nitrogen conditions were used to isolate determinate nodules

from their roots after inoculation with *Rhizobium loti* NZPP3230 (Strozycki et al., 2000).

Production of Recombinant *Msca1* Protein and Antibodies

A complete Msca1 cDNA was cloned at the 5′ end of the multicloning site of the expression vector pQE23 (Qiagen, France) in phase with the first ATG of the vector, and used to transform competent M15 bacteria. This strategy allowed production of a recombinant Msca1 protein tagged with six additional His residues at its N-terminal region, which was purified in one step with an affinity column (according to the manufacturer's instructions, Qiagen). It was usual that 2 mg of purified protein per 200 mL of an overnight-induced culture were obtained.

Antibodies were prepared as described by Vidal et al. (1980) and redissolved in 50 mM sodium phosphate buffer at pH 7.2, 0.9% (w/v) NaCl. Antibodies raised against a specific synthetic peptide from the potato leaf CA were characterized in Rumeau et al. (1996).

Protein Extraction, CA Activity, and Western Blotting

Plant materials were ground in liquid nitrogen and homogenized in microcentrifuge tubes using a plastic pestle (homogenization buffer: 100 mM sodium phosphate, pH 7.2 and 14 mM β-mercaptoethanol; 0.2 mL of buffer per 100 mg of ground material). Samples were centrifuged at 10,000 rpm at 4°C for 15 min and supernatants were used as total soluble protein extracts. Protein content was determined by the Bradford assay (Bio-Rad, Hercules, CA).

Denaturing SDS-PAGE (Laemmli, 1970) was performed using a 4% (w/v) stacking gel and a 10% (w/v) separating gel. Native PAGE was carried out by using a 4% (w/v) stacking gel and a 7% (w/v) separating gel. CA activity was detected as a local alkaline-acidic pH change after incubation of the gel in a tank containing dry ice in the presence of bromothymol blue, as described by Tashian (1969). Separated proteins were electrotransferred to a nylon membrane using a transfer apparatus (Bio-Rad) at 200 mA for 4 h (SDS-PAGE) or overnight (native PAGE). The transfer buffer consisted of 25 mM Tris [tris(hydroxymethyl)-aminomethane], pH 8.3, 192 mM Gly, and 20% (v/v) ethanol. After blocking, protein bands were visualized by incubating the membrane with antiserum diluted 1:400 and anti-rabbit alkaline phosphatase antibody (Sigma, St. Louis) at a final dilution of 1:30,000. For staining, nitroblue tetrazolium salt and 5-bromo-4-chloro-3-indolyl-phosphate tablets (Boehringer Mannheim, Basel) were used.

Light Microscopy

Nodules were freshly collected, placed in a fixative solution (4% [w/v] paraformaldehyde and 1% [w/v] glutaraldehyde in 100 mM sodium phosphate buffer, pH 7.2) for 4 h under vacuum, and dehydrated in an ethanol series. *M. truncatula* nodules were embedded in paraffin or methacrylate as described previously (Coba de la Peña et al., 1997; Evans et al., 1997, respectively). *L. japonicus* nodules were embedded in methacrylate. Preparation of paraffin-embedded alfalfa nodules grown at different oxygen conditions has been described previously (Wycoff et al., 1998). Semithin sections (8-μm) were treated to eliminate the paraffin or the resin and then treated in the same way. Unspecific sites were blocked by incubation in Tris-buffered saline (Tris, 25 mM, pH 7.5 and NaCl, 150 mM) plus 2.5% (w/v) bovine serum albumin for 30 min at room temperature. Sections were then incubated with the appropriate antibody (dilution 1:250) overnight at 4°C. After washing, sections were incubated with a secondary anti-rabbit antibody conjugated to the Cy3-conjugated AffiniPure goat anti-rabbit IgG (excitation wavelength of 570 nm and an emission wavelength of 570 nm; Jackson ImmunoResearch Laboratories, Baltimore, MD). After washing in Tris-buffered saline, the slides were mounted in Cityfluor medium. Observations were made with an epifluorescence microscope (Polyvar, Reichert-Jung, Vienna). Autofluorescence images were obtained with a filter set band pass 395 to 446 nm excitation filter, a DS 460 dichroic mirror, and a long pass 471 nm stop filter. The fluorescence due to the dye was observed with a filter set band pass (546 nm) and a long pass (590 nm) stop filter. Photographs were obtained using Kodak Ektachrome films (Rochester, NY).

Confocal Microscopy

Confocal images were obtained with a confocal microscope (Sarastro 2000, Molecular Dynamics, Sunnyvale, CA) with a 514-nm excitation and a 600-nm emission filter. Serial optical sections of 1 mm were taken for each sample and those containing most of the red signal were selected. Fifteen serial sections of 0.5 mm each containing most of the red signal were selected and projected into one two-dimensional section. A given surface (3,500–6,600 μm^2) in either the IC (to measure *Msca1*-dependent fluorescence) or the IZ (considered as background level) was chosen for calculations of relative fluorescence intensities. In this way the intensity of the red, Cy3-dependent signal by area unit in the final projection could be measured. To compare the amounts of fluorescence intensities in the IC in the different treatments, the values (intensity per area) obtained in the IC region were compared with those measured in the adjacent infected cells. Immunolocalization treatments between the different antiserum were done on serial sections of the same nodules with either the pre-immune or the different anti-CA antibodies.

ACKNOWLEDGMENTS

We thank Dr. Gilles Peltier (Department of Ecophysiologie Végétale et Microbiologie, Commissariat à l'Energie Atomique- Centre National de la Recherche Scientifique, Cadarache, France) for the kind gift of anti-potato leaf CA antibodies and an anonymous reviewer who made numerous suggestions to help in the improvement of the manuscript. The help of Nathalie Mansion (Institut des Sciences Végétales, Centre National de la Recherche Scientifique,

Gif-sur-Yvette, France) for the photographic work is also acknowledged.

Received May 31, 2000; accepted August 3, 2000.

LITERATURE CITED

Arrese-Igor C, Royuela M, de Lorenzo C, de Felipe MR, Aparicio-Tejo PM (1993) Effect of low rhizosphere oxygen on growth, nitrogen fixation and nodule morphology in lucerne. Physiol Plant **89:** 55–63

Atkins CA (1974). Occurrence and some properties of carbonic anhydrases from legume root nodules. Phytochemistry **13:** 93–98

Atkins CA, Patterson BD, Graham D (1972) Plant carbonic anhydrases: I. Distribution among species. Plant Physiol **50:** 214–217

Badger MR, Price GD (1994) The role of carbonic anhydrase in photosynthesis. Annu Rev Plant Physiol Plant Mol Biol **45:** 369–392

Batut J, Boistard P (1994) Oxygen control in *Rhizobium*. Antonie Leeuwenhoek **66:** 129–150

Beckett PM, Armstrong W, Justin S, Armstrong J (1988) On the relative importance of convective and diffusive gas flows in plant aeration. New Phytol **110:** 463–468

Burnell JN, Gibbs MJ, Mason JG (1990) Spinach chloroplastic carbonic anhydrase: nucleotide sequence analysis of cDNA. Plant Physiol **92:** 37–40

Cavallaro A, Ludwig M, Burnell J (1994) The nucleotide sequence of a complementary DNA encoding *Flaveria bidentis* carbonic anhydrase. FEBS Lett **350:** 216–218

Coba de la Peña T, Frugier F, McKhann HI, Bauer P, Brown S, Kondorosi A, Crespi M (1997) A carbonic anhydrase gene is induced in the nodule primordium and its cell-specific expression is controlled by the presence of *Rhizobium* during development. Plant J **11:** 407–420

Crespi MD, Jurkevitch E, Poiret M, D'Aubenton-Carafa Y, Petrovics G, Kondorosi E, Kondorosi A (1994) enod40, a gene expressed during nodule organogenesis, codes for a non-translatable RNA involved in plant growth. EMBO J **13:** 5099–5112

Drevon JJ, Deransart C, Fleurat-Lessard P, Jaillard B, Ndjiondjop MN, Payre H, Ribet J, Roy G, Serraj R (1995) Is the symbiotic fixation osmoregulated by reversible contraction of cells in the legume-nodule inner cortex? *In* IA Tikhonovitch, NA Provorov, VI Romanov, WE Newton, eds, Nitrogen Fixation: Fundamentals and Applications. Kluwer Academic Publishers, Dordrecht, The Netherlands, p 598

Evans DE, Clay PJ, Attree S, Fowke LC (1997) Visualization of Golgi apparatus in methacrylate embedded conifer embryo tissue using the monoclonal antibody JIM 84. Cell Biol Int **21:** 295–302

Fett JP, Coleman JR (1994) Characterization and expression of two cDNAs encoding carbonic anhydrase in *Arabidopsis thaliana*. Plant Physiol **105:** 707–713

Hatch MD, Burnell JN (1990) Carbonic anhydrase activity in leaves and its role in the first step of C4 photosynthesis. Plant Physiol **93:** 825–828

Hunt S, Denison RF, King BJ, Kouchi H, Tajima S, Layzell DB (1990) An osmotic mechanism for diffusion barrier regulation in soybean nodules. *In* PM Gresshoff, LE Roth, G. Stacey, WE Newton, eds, Nitrogen Fixation: Achievements and Objectives. Chapman & Hall, New York, pp 352–360

Hunt S, Gaito ST, Layzell DB (1988) Model of gas exchange and diffusion in legume nodules: II. Characterization of the diffusion barrier and estimation of the concentrations of CO_2, H_2 and N_2 in the infected cells. Planta **173:** 128–141

Hunt S, Layzell DB (1993) Gas exchange of legume nodules and the regulation of nitrogenase activity. Annu Rev Plant Physiol Plant Mol Biol **44:** 483–511

Iannetta PPM, James EK, Sprent JI, Minchin JR (1995) Time course of changes involved in the operation of the oxygen diffusion barrier in white lupin nodules. J Exp Bot **46:** 565–575

Iwasaki I, Arata H, Kijama H, Nishimura M (1992) Two types of channels involved in the malate ion transport across the tonoplast of a crassulacean acid metabolism plant. Plant Physiol **98:** 1494–1497

King BJ, Layzell DB, Canvin DT (1986) The role of dark carbon dioxide fixation in root nodules of soybean. Plant Physiol **81:** 200–205

Kuzma MM, Hunt S, Layzell DB (1993) Role of oxygen in the limitation and inhibition of nitrogenase activity and respiration rate in individual soybean nodules. Plant Physiol **101:** 161–169

Laemmli UK (1970) Cleavage of structural proteins during the assembly of the head of bacteriophage T4. Nature **227:** 680–685

Layzell DB, Hunt S, Palmer GR (1990) Mechanism of nitrogenase inhibition in soybean nodules. Plant Physiol **92:** 1101–1107

Ludwig M, von Caemmerer S, Price D, Badger MR, Furbank RT (1998) Expression of tobacco carbonic anhydrase in the C4 dicot *Flaveria bidentis* leads to increased leakiness of the bundle sheath and a defective CO_2-concentrating mechanism. Plant Physiol **117:** 1071–1081

Majeau N, Coleman JR (1991) Isolation and characterization of a cDNA coding for pea chloroplastic carbonic anhydrase. Plant Physiol **95:** 264–268

Majeau N, Coleman JR (1994) Correlation of carbonic anhydrase and ribulose-1,5-bisphosphate carboxylase/oxygenase expression in pea. Plant Physiol **104:** 1393–1399

Miller SS, Boylan KLM, Vance CP (1987) Alfalfa root nodule CO_2 fixation: III. Immunological studies of nodule phospho*enol*pyruvate carboxylase. Plant Physiol **84:** 501–508

Pathirana MS, Samac DA, Roeven R, Yoshioka H, Vance CP, Gantt JS (1997) Analyses of phospho*enol*pyruvate carboxylase gene structure and expression in alfalfa nodules. Plant J **12:** 293–304

Price G, Caemmerer S, Evans J, Yu JW, Loyd J, Oja V, Kell P, Harrison K, Gallagher A, Badger M (1994) Specific reduction of chloroplast carbonic anhydrase activity by antisense RNA in transgenic tobacco plants has a minor

effect on photosynthetic CO_2 assimilation. Planta **193:** 331–340

Raines CA, Horsnell P, Holder C, Lloyd JC (1992) *Arabidopsis thaliana* carbonic anhydrase: cDNA sequence and effect of CO_2 on mRNA levels. Plant Mol Biol **20:** 1143–1148

Rumeau D, Cuiné S, Fina L, Gault N, Nicole M, Peltier G (1996) Subcellular distribution of carbonic anhydrase in *Solanum tuberosum* L. leaves: characterization of two compartment-specific isoforms. Planta **199:** 79–88

Sheehy JE, Bergersen FJ, Minchin FR, Witty JF (1987) A simulation study of gaseous diffusion resistance, nodule pressure gradients and biological nitrogen fixation in soybean nodules. Ann Bot **60:** 345–351

Strozycki PM, Karlowski WM, Dessaux Y, Petit A, Legocki AB (2000) Lupin leghemoglobin: I. Expression in transgenic lotus and tobacco tissues. Mol Gen Genet **263:** 173–182

Sültemeyer D, Schmidt C, Fock HP (1993) Carbonic anhydrases in higher plants and aquatic microorganisms. Physiol Plant **88:** 179–190

Tashian RE (1969) The esterases and carbonic anhydrases in human erythrocytes. *In* JJ Yunis, ed, Biochemical Methods in Red Cell Genetics. Academic Press, New York, pp 307–318

Thumfort PP (1996) Nitrogen fixation and oxygen in legume root nodules: the mathematical modelling of oxygen diffusion into infected cells. PhD thesis. The University of Western Australia, Perth

Thumfort PP, Layzell DB, Atkins CA (1999) Diffusion and reaction of oxygen in the central tissue of ureide-producing legume nodules. Plant Cell Environ **22:** 1351–1365

Vance CP, Gantt JS (1992) Control of nitrogen and carbon metabolism in root nodules. Physiol Plant **85:** 266–274

Vance CP, Gregerson RG, Robinson DL, Miller SS, Gantt JS (1994) Primary assimilation of nitrogen in alfalfa nodules: molecular features of the enzymes involved. Plant Sci **101:** 51–64

Vessey JK, Waterer J (1992) In search of the mechanism of nitrate inhibition of nitrogenase activity in legume nodules: recent developments. Physiol Plant **84:** 171–176

Vidal J, Godbillon G, Gadal P (1980) Recovery of active highly purified phospho*enol*pyruvate carboxylase from specific immunoabsorbent column. FEBS Lett **118:** 31–34

Witty JF, Minchin FR, Skot L, Sheehy JE (1986) Nitrogen fixation and oxygen in legume root nodules. *In* BJ Miflin, HF Miflin, eds, Oxford Surveys of Plant Molecular and Cell Biology, Vol 3. Oxford University Press, Oxford, pp 275–314

Wycoff KL, Hunt SH, Gonzales MB, Van den Bosch KA, Layzell DB, Hirsch AM (1998) Effects of oxygen on nodule physiology and expression of nodulins in alfalfa. Plant Physiol **117:** 385–395